Interleukin-13 Induces Tissue Fibrosis by Selectively Stimulating and Activating Transforming Growth Factor β_1

Chun Geun Lee,[1] Robert J. Homer,[2,3] Zhou Zhu,[1] Sophie Lanone,[1]
Xiaoman Wang,[1] Victor Koteliansky,[4] J. Michael Shipley,[5]
Philip Gotwals,[4] Paul Noble,[1] Qingsheng Chen,[1] Robert M. Senior,[5]
and Jack A. Elias[1]

[1]*Yale University School of Medicine, Section of Pulmonary and Critical Care Medicine, Department
of Internal Medicine and the* [2]*Department of Pathology, New Haven, CT 06520*
[3]*Pathology and Laboratory Medicine Service, VA-CT Health Care System, West Haven, CT 06516*
[4]*Biogen, Inc., Cambridge, MA 02142*
[5]*Washington University School of Medicine, Section of Pulmonary and Critical Care Medicine,
Barnes-Jewish Hospital, St. Louis, MO 63110*

Abstract

Interleukin (IL)-13 is a key mediator of tissue fibrosis caused by T helper cell type 2 inflammation. We hypothesized that the fibrogenic effects of IL-13 are mediated by transforming growth factor (TGF)-β. To test this hypothesis we compared the regulation of TGF-β in lungs from wild-type mice and CC10-IL-13 mice in which IL-13 overexpression causes pulmonary fibrosis. IL-13 selectively stimulated TGF-β_1 production in transgenic animals and macrophages were the major site of TGF-β_1 production and deposition in these tissues. IL-13 also activated TGF-β_1 in vivo. This activation was associated with decreased levels of mRNA encoding latent TGF-β–binding protein-1 and increased mRNA encoding urinary plasminogen activator, matrix metalloproteinase (MMP)-9, and CD44. TGF-β_1 activation was abrogated by the plasmin/serine protease antagonist aprotinin. It was also decreased in progeny of crosses of CC10-IL-13 mice and MMP-9 null mice but was not altered in crosses with CD44 null animals. IL-13–induced fibrosis was also significantly ameliorated by treatment with the TGF-β antagonist soluble TGFβR-Fc (sTGFβR-Fc). These studies demonstrate that IL-13 is a potent stimulator and activator of TGF-β_1 in vivo. They also demonstrate that this activation is mediated by a plasmin/serine protease- and MMP-9–dependent and CD44-independent mechanism(s) and that the fibrogenic effects of IL-13 are mediated, in great extent, by this TGF-β pathway.

Key words: lung • plasmin • matrix metalloproteinase-9 • CD44 • asthma

Introduction

Tissue fibrosis is a well-documented consequence of Th2 cytokine-dominated inflammatory responses. This is nicely illustrated in asthma where Th2-dominated inflammation is the cornerstone of the disorder (1, 2) and airway remodeling with subepithelial fibrosis are believed to be adverse consequences of this inflammatory response (for a review, see reference 3). Th2 inflammation also plays a central role in the pathogenesis of a variety of other fibrotic disorders including progressive systemic sclerosis (4–6), idiopathic pulmonary fibrosis (IPF*; references 5–8), radiation-induced pulmonary fibrosis (9), chronic lung allograft rejection (10), bleomycin lung (11), and hepatic fibrosis (12–15). In vitro polarized Th2 cells also induce tissue fibrosis when passively transferred and activated in vivo (16). In contrast, Th1 cytokine-dominated responses eventuate in tissue fibrosis less frequently and IFN-γ, the prototypic Th1 cytokine, has a variety of antifibrotic effector proper-

Abbreviations used in this paper: BAL, bronchoalveolar lavage; IPF, idiopathic pulmonary fibrosis; ISH, in situ hybridization; LAP, latency–associated peptide; LTBP, latent TGF-β–binding protein; MMP, matrix metalloproteinase; PAI, plasminogen activator inhibitor; RT, reverse transcription; s, soluble; uPA, urokinase type plasminogen activator; WT, wild-type.

Address correspondence to Jack A. Elias, Yale University School of Medicine, Section of Pulmonary and Critical Care Medicine, Dept. of Internal Medicine, 333 Cedar St. - 105 LCI, New Haven, CT 06520-8057. Phone: 203-785-4163; Fax: 203-785-3826; E-mail: jack.elias@yale.edu

ties and has been shown to be a useful antifibrotic agent in murine and human pulmonary and renal fibrotic disorders (8, 17–19). As a result of these findings, the "type 2 cytokine hypothesis of fibrosis" has been formulated which suggests that fibrosis occurs when cytokine balance shifts in a Th2 (type 2) direction (19). Surprisingly, the mechanism(s) by which Th2 inflammation generates tissue fibrosis is poorly understood. In addition, although it is assumed in this hypothesis that Th2 cytokines induce fibrosis via pathways that are independent of known mediators of fibrosis such as TGF-β, the validity of this assumption has not been adequately assessed.

IL-13 is a pleiotropic cytokine produced by a gene on chromosome 5 at q31 that is elaborated in significant quantities by appropriately stimulated Th2 cells (20, 21). A variety of lines of evidence have demonstrated that IL-13 is an important mediator in the pathogenesis of asthma (22–25). IL-13 has also been implicated in the pathogenesis of hepatic fibrosis, progressive systemic sclerosis, pulmonary fibrosis, and nodular sclerosing Hodgkin's disease (4, 12, 13, 26–28). In these diseases IL-13 is felt to contribute to the pathogenesis of tissue fibrosis. This is based on studies from our laboratory that demonstrated that the transgenic overexpression of IL-13 in the murine airway causes subepithelial airway fibrosis that is similar, in many ways, to the fibrotic response seen in remodeled human asthmatic airways (3, 25). It is also based on studies that demonstrate that IL-13 is the primary cytokine responsible for hepatic fibrosis in murine schistosomiasis and that IL-13 is a potent stimulator of fibroblast proliferation and collagen production in vitro (12, 13, 29, 30). Surprisingly, the mechanism of IL-13–induced fibrosis has not been further defined. In addition, the relationship between IL-13 and TGF-β cytokines, which are also dysregulated in many of these disorders, have not been elucidated.

We hypothesized that IL-13 mediates its fibrogenic effects in the lung and other organs by altering TGF-β cytokine homeostasis. To test this hypothesis we characterized the regulation and role of TGF-β moieties in lungs from wild-type (WT) mice and transgenic CC10-IL-13 mice in which the overexpression of IL-13 causes airway and parenchymal fibrosis (25). These studies demonstrate that IL-13 selectively stimulates and activates TGF-β_1. They also define the mechanism of this TGF-β_1 activation and demonstrate that the fibrotic effects of IL-13 are mediated, in great extent, by this TGF-β_1 induction and activation pathway.

Materials and Methods

Genetically Manipulated Mice. CC10-IL-13 mice, mice with homozygous null mutations of matrix metalloproteinase (MMP)-$9^{-/-}$, and mice with homozygous null mutations of CD44 (CD44$^{-/-}$) were used in these studies. In the CC10-IL-13 mice, the Clara cell 10-kDa (CC10) promoter was used to constitutively overexpress IL-13 in a lung-specific fashion. The methods that were used to generate these mice in our laboratory and the organ specificity of transgene expression, levels of bronchoalveo-

lar lavage (BAL) IL-13, and the phenotype of these animals have been described previously (25). The MMP-$9^{-/-}$ mice were also generated in our laboratories (31). MMP-9 is inactivated in these mice as a result of the insertion of NEO genes in exon-2 of each MMP-9 allele. CD44$^{-/-}$ mice were obtained from T. Mak (Amgen Institute, Toronto, Canada; reference 32). CC10-IL-13 mice with homozygous null mutations of MMP-9 (CC10-IL-13/MMP-$9^{-/-}$) or CD44 (CC10-IL-13/CD44$^{-/-}$) were generated by breeding CC10-IL-13 transgene (+) mice with MMP-$9^{-/-}$ or CD44$^{-/-}$ animals. Unless otherwise indicated, WT littermates (+/+) were used as negative controls.

BAL. After anesthesia, a median sternotomy was performed and the trachea was exposed by blunt dissection. A 22-gauge catheter was inserted into the trachea, and BAL was performed by instilling 1 ml of PBS into the trachea and gently aspirating back. This was repeated twice. The BAL samples from each animal were pooled and centrifuged. Differential cell counts were performed on the pellet and the supernatant was stored at $-20°C$ until used.

Histologic Evaluation. Histologic evaluation was performed as described previously (25, 33, 34). In brief, animals were killed, a median sternotomy was performed, and right heart perfusion was accomplished with calcium- and magnesium-free PBS to clear the pulmonary intravascular space. The heart and lung were then removed en bloc, fixed to pressure (25 cm) with neutral buffered formalin, incubated overnight in formalin, embedded in paraffin, sectioned, and stained. Hematoxylin and eosin, Mallory's Trichrome, and Sirius red staining were performed in the Research Pathology Laboratory at Yale University, New Haven, CT.

Treatment with Soluble TGF-β Type II Receptor-Fc and Aprotinin. The role of TGF-β was assessed using soluble TGFβR-Fc (sTGFβR-Fc). This TGF-β antagonist contains a soluble TGF-β type II receptor attached to the Fc fragment of human IgG. The generation protocols and in vitro and in vivo efficacy of this construct have been described previously (35, 36). It was administered to IL-13 transgene (+) and littermate control mice in PBS (2 mg/kg) by intraperitoneal injection every other day for 8 wk, starting when the mice were 4 wk old. An equivalent dose of pooled human IgG was used as a control.

Aprotinin from bovine lung (6618 KIU/mg) was purchased from ICN Inc. It was administered to IL-13 transgene (+) mice and littermate controls (500 μg/mouse) by intraperitoneal injection every day for 4 wk starting when the mice were 4 wk of age. An equivalent dose of PBS was administered according to the same schedule as a vehicle control.

mRNA Analysis. mRNA levels were assessed using reverse transcription (RT)-PCR and ribonuclease protection assays as described previously by our laboratories (33, 37). In these experiments, total lung RNA was obtained using TRIzol reagent (Life Technologies) as per the manufacturer's instructions followed by treatment with DNase I (Ambion, Inc.). In the RT-PCR assays, 0.5 μg of RNA was reverse transcribed to cDNA and gene-specific primers (Table 1) were used to amplify selected regions of each target moiety. The primers and optimum conditions used in the reactions were designed according to published sequences. The whole reaction was performed in a 25 μl volume using an Access RT-PCR kit purchased from Promega according to the manufacturer's instructions. All primers were synthesized at the Yale Oligonucleotide Synthesis Laboratory. To verify that equal amounts of undegraded RNA were added in each RT-PCR reaction, β-actin was used as an internal standard. Amplified PCR products were detected using 1.2% agarose ethidium bromide gel

Table I. *Primer Sequences and RT-PCR Conditions*

Gene	s/as	Primer Sequences (5′ to 3′)	Anneal. Tm.	Cycle	Product Size (bp)	GenBank Accession Number
LTBP-1	s	GGTGTGTGGATGTGAACGAG	60°C	30	447	AF022889
	as	CTCCAAACAGCAAGCATTCA				
CD36	s	GCAAAGAAGGAAAGCCTGTG	60°C	30	337	L23108
	as	TCTACCATGCCAAGGAGCTT				
TSP-1	s	GACGTCGATGAGTGCAAAGA	60°C	27	532	M87276
	as	AGTCATACTGGGCTGGGTTG				
INT-β_6	s	AGGGGTGACTGCTATTGTGG	60°C	30	423	AF115376
	as	GGCACCAATGGCTTTACACT				
uPA	s	CCTACAATGCCCACAGACCT	60°C	25	471	NM-008873
	as	GCTGCTCCACCTCAAACTTC				
PAI-1	s	TCATCAATGACTGGGTGGAA	60°C	30	539	M33960
	as	CTGCTCTTGGTCGGAAAGAC				
MMP-9	s	CCATGAGTCCCTGGCAG	58°C	30	505	X72795
	as	ATGACAATGTCCGCTTCG				
CD-44	s	GAGGATTCATCCCAACGCTA	60°C	25	499	M27129
	as	GGTCACTCCACTGTCCTGGT				
β-actin	s	GTGGGCCGCTCTAGGCACCA	65°C	20	241	X03672
	as	TGGCCTTAGGGTTCAGGGGG				

Anneal. Tm., annealing temperature; as, antisense; INT, integrin; s, sense; TSP, thrombospondin.

electrophoresis, quantitated electronically, and confirmed by nucleotide sequencing. Ribonuclease protection assays were performed using the RiboQuant In Vitro Transcription kit (BD PharMingen) according to manufacturer's instructions.

Quantification of TGF-β1. The levels of immunoreactive TGF-β_1 and TGF-β_2 were determined with cytokine-specific commercial ELISA kits as per the manufacturer's instructions (R&D Systems).

Immunohistochemistry. Immunostains for TGF-β_1 was performed on paraffin-embedded tissues that had been fixed in either Streck's tissue fixative or neutral buffered 4% formalin. After sectioning the tissues were rehydrated, endogenous peroxidase was blocked by quenching with H_2O_2 and methanol and the tissues were treated in a microwave oven in the presence of citrate buffer (10 mM, pH 6.0) for 9 min (3 cycles of 3 min each). After preblocking with Dako blocking reagent (Dako) for 15 min, polyclonal rabbit anti–TGF-β_1 antibody (Santa Cruz Biotechnology, Inc.) was applied at a 1:100 dilution. In experiments designed to see if an appropriate peptide competed for antibody binding, the anti–TGF-β_1 antiserum was preincubated with murine TGF-β_1 (R&D Systems) at a 1:1 molar ratio for 2 h before it was applied to the tissues. After overnight incubation at 4°C, the tissues were rinsed with PBS/0.1% Tween 20 and Envision (Dako) peroxidase coupled anti–rabbit secondary reagent was applied for 30 min. The slides were then washed, 3,3′diaminobenzidine was applied for 5 min, and the tissues were counterstained with hematoxylin.

In Situ Hybridization. Lung tissue was fixed in formaldehyde and processed into paraffin. 5 μ sections were cut, deparaffinized, treated with proteinase K (20 μg/ml) for 20 min at 37°C followed by 0.1 M triethylnolamine/0.25% acetic anhydride, pH

8.0, for 10 min at room temperature, and then rinsed in PBS. The mouse TGF-β_1 probe (containing the segment from the mouse TGF-β_1 sequence between base pairs 1027–1465; GenBank Accession, NM-011577) was placed in a pBluescript II KS phagemid (Stratagene) between T7 and T3 promoter sites. Sense and antisense RNA probes were generated, labeled with a digoxigenin RNA labeling kit (Roche), denatured at 65°C, added to commercially available hybridization buffer (Ambion) at 6 ng/μl, and the hybridization mixture was incubated with tissue overnight at 52°C. The tissues were then washed twice with 4×SSC for 5 min at room temperature, twice with 2×SSC for 10 min at 37°C, and incubated with RNase A (10 μg/ml) for 45 min at 37°C. This was followed by 2 10-min washes in 2×SSC at room temperature and 3 20-min washes in 0.2×SSC at 50°C. Probe was detected by overnight incubation with sheep antibodies to digoxigenin-labeled with alkaline phosphatase (Roche) followed by 4-nitroblue tetrazolium chloride/5-bromo-4-chloro-3-indoylphosphate (BCIP/NBT) as described by the manufacturer.

TGF-β Bioassay. To measure the bioactivity of TGF-β in BAL fluids, we used mink lung epithelial cells permanently transfected with a construct containing the TGF-β responsive human plasminogen activator inhibitor (PAI)-1 promoter fused to a luciferase reporter gene (TMLC, a gift from John Munger, NYU Medical Center, New York, NY). These cells were seeded into wells of 12-well tissue culture plates (10^5 cells per well per milliliter) in DMEM supplemented with 10% FCS and allowed to attach for 5 h. They were then washed and incubated in triplicate in mixtures containing 200 μl of BAL fluid and 800 μl of assay medium (DMEM with 2.5% FCS). These incubations were performed in the presence and absence of saturating quantities of neutralizing antibodies specific for TGF-β_1, TGF-β_2, or TGF-β_3

(R&D Systems). The luciferase activities in these cells were measured 16 h later using the Luciferase Assay System (Promega) according to the manufacturer's instructions. The bioactivity attributed to TGF-β_1 (TGF-β_1 bioactivity) was defined as the difference in the luciferase activities of identical cells incubated in the absence and presence of anti–TGF-β_1.

Western Blot Analysis. BAL fluids were concentrated fivefold using Centricon 10 concentrators (Amicon). Equal volumes of test and control samples were fractionated on 15% SDS-PAGE gels under reducing conditions and transferred to PVDF membranes (Millipore). The membranes were then blocked with 5% nonfat dry milk, washed three times with PBS/0.1% Tween 20, and incubated for 1 h at room temperature in a 1:200 dilution of rabbit polyclonal anti–TGF-β_1, anti–TGF-β_2, or anti–TGF-β_3 antibodies (Santa Cruz Biotechnology, Inc.). After washing with PBS/ 0.1% Tween 20, they were incubated for 1 h with a horseradish peroxidase-conjugated donkey anti–rabbit antibody (Amersham Pharmacia Biotech), rewashed in PBS/0.1% Tween 20, and protein bands were detected using the ECL Western blot detection system (Amersham Pharmacia Biotech).

Collagen Assay. Total lung collagen content was determined by quantifying total soluble collagen using the Sircol Collagen Assay kit (Biocolor) according to the manufacturer's instructions. Briefly, lungs were homogenized in 5 ml of 0.5 M acetic acid containing 1 mg pepsin (Sigma-Aldrich)/10 mg tissue residue. Each sample was incubated for 24 h at 4°C with stirring. After centrifugation, 100 μl of each supernatant was assayed. 1 ml of Sircol dye reagent that specifically binds to collagen was then added to each sample and mixed for 30 min. After centrifugation the pellet was suspended in 1 ml of alkali reagent (0.5 M NaOH) included in the kit and optical density evaluated at 540 nm with a spectrophotometer. The values in the test samples were compared to the values obtained with collagen standard solutions provided by the manufacturer that were used to construct a standard curve.

Picosirius Red Staining and Evaluation. Collagen content was assessed using Picosirius red staining. This approach was chosen because it accurately reflects organ collagen content assessed with hydroxyproline assays (38, 39) and allows areas of localized collagen accumulation to be specifically evaluated. In these assays, sections of lung are stained with Sirius red as described previously (40). For examination of lung parenchyma, the tissue was examined under polarized light with an Olympus BH-2 microscope with an original magnification: 2× objective. This magnification allows virtually the entire lung section to be acquired for analysis using 4–6 fields. Image acquisition was performed with a DXC-970MD Sony video camera attached to a iXTV video capture card (IXMICRO) in a G3 Macintosh (Apple Computer) using software included with the card. Images are captured as grey scale TIFF encoded video clips. These are opened in NIH Image and averaged to reduce noise. Images are then subject to 2-D rolling ball background subtraction to make the background uniform. Areas of parenchyma are manually outlined to exclude airways and large vessels, then thresholded. The number of white versus total pixels are then recorded. The total number of white pixels versus total pixels examined is a reflection of collagen density.

For examination of airway fibrosis, images were acquired with an original objective: 4× objective. Only airways that were oval or circular and are outside the central bronchovascular sheath were analyzed. Each field was acquired as a regular color image as well as a polarized image. Images were opened within NIH Image. The airway was outlined using the color image to determine area and minor axis. The same airway was outlined in the polar-

ized image and subject to thresholding to determine the number of white pixels. Data was expressed as area of collagen versus total airway area.

Statistics. Normally distributed data are expressed as means ± SEM and assessed for significance by Student's *t* test or ANOVA as appropriate. Data that were not normally distributed were assessed for significance using the Wilcoxon rank sum test.

Results

Effect of IL-13 on TGF-β_1 Production. Pulmonary fibrosis was a prominent finding in CC10-IL–13 mice. As previously reported, subepithelial and adventitial airway fibrosis were readily appreciated in 1–mo-old animals (25). This response continued to progress over the life of the mouse. By the time the mice were 2–3 mo of age, parenchymal fibrosis was also appreciated (Fig. 1). To gain insight into the mechanisms of this fibrotic response, studies were undertaken to determine if IL-13 stimulated the production of TGF-β moieties in the murine lung. Our initial studies used ribonuclease protection assays to compare the levels of TGF-β_1, TGF-β_2, and TGF-β_3 mRNA in lungs from transgene (−) and transgene (+) animals. As can be seen in Fig. 2, IL-13 caused an impressive increase in the levels of mRNA encoding TGF-β_1. Comparable increases in the levels of mRNA encoding TGF-β_2 were not appreciated. In addition, the levels of TGF-β_3 in lungs from transgene (+) mice were lower than the levels in their transgene (−) littermate controls (Fig. 1).

Studies were next undertaken to determine if the increased levels of TGF-β_1 mRNA in lungs from transgene (+) mice were associated with increased levels of BAL fluid TGF-β_1 protein. Using an ELISA assay that detects bioactive cytokine, TGF-β_1 was not detected in significant quantities in acid-treated BAL fluids from transgene (−) animals (Fig. 3 A). Significantly increased levels of TGF-β_1 were noted in acid-treated BAL from 1–mo-old transgene (+) animals and the levels of BAL TGF-β_1 continued to increase as the animals aged (Fig. 3 A). In contrast, TGF-β_2 was not detected by ELISA in BAL fluids from transgene (−) or (+) animals (data not shown). In accord with these findings, TGF-β_1 monomers were readily detected in immunoblots performed with acid-treated BAL fluids from transgene (+) mice but were not readily apparent in BAL fluids from transgene (−) littermate controls (see Fig. 3 B). Comparable alterations in the levels of TGF-β_2 and TGF-β_3 proteins were not noted in comparisons of immunoblots from acid–activated BAL fluids from transgene (+) and (−) mice (data not shown). When viewed in combination, these findings demonstrate that IL-13 selectively stimulates TGF-β_1 mRNA accumulation and protein production in the murine lung.

Localization of TGF-β_1 in IL-13 Transgenic Mice. To gain insight into the mechanism(s) of TGF-β_1 induction, immunohistochemistry and in situ hybridization (ISH) were used to localize and define the sites of TGF-β_1 production in lungs from transgene (−) and transgene (+) animals. TGF-β_1 protein and mRNA were readily apparent in
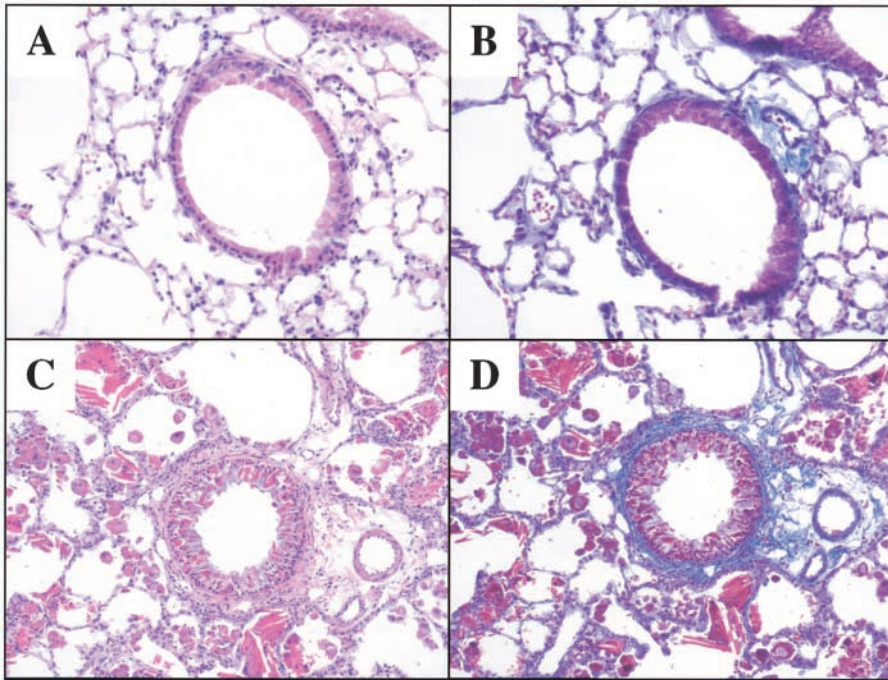
Figure 1. Histologic responses in CC10-IL-13 mice. H&E stains are used in A and C to compare the histologic features of WT littermate control mice and 3-mo-old CC10-IL-13 transgene (+) mice respectively. Trichrome stains are used in B and D to compare the collagen in WT littermate control mice and 3-mo-old transgene (+) animals respectively. All figures are at original magnification: 20×. Collagen stains blue in these panels.

airway epithelial cells in lungs from transgene (−) animals. Low levels of TGF-β, mRNA, and protein were also noted in some alveolar macrophages (Figs. 4 and 5 and data not shown). In lungs from IL-13 transgene (+) mice impressive increases in macrophage TGF-β$_1$ mRNA and protein were readily apparent. Lower levels of TGF-β$_1$ mRNA and protein could also be appreciated in type II alveolar epithelial cells, airway epithelial cells, and occasionally in eosinophils from these transgene (+) animals (Figs. 4 and 5 and data not shown). In these immunohistochemical evaluations, preincubation of our primary antibody with TGF-β$_1$ peptide effectively abrogated the detection of TGF-β$_1$ in these tissues (Fig. 4). In the ISHs, significant staining with the sense probe was not noted (Fig. 5). This demonstrates the specificity of these approaches. Thus, lung macrophages are the major sites of production and storage, and airway and alveolar epithelial cells and eosinophils are lesser sites of production and storage of TGF-β$_1$ in lungs from IL-13 transgene (+) animals.
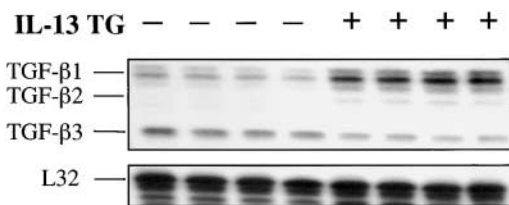
Effect of IL-13 on TGF-β$_1$ Activation. TGF-β cytokines are produced as biologically inactive moieties with the TGF-β$_1$ dimer bound to its propeptide, latency-associated peptide (LAP). They exert their tissue effects after activation, a complex process that likely involves proteolysis
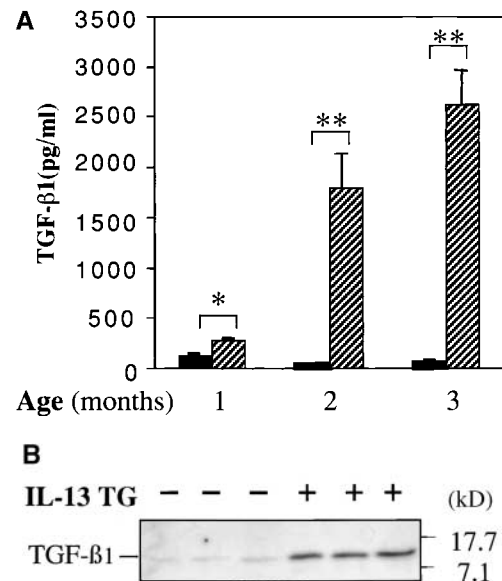

Figure 2. Effect of IL-13 on TGF-β cytokine mRNA. Whole lung RNA from IL-13 transgene (+) mice and transgene (−) littermate controls were obtained. The levels of mRNA encoding TGF-β$_1$, TGF-β$_2$, TGF-β$_3$, and L32, the housekeeping control gene, were assessed using ribonuclease protection assays. Each lane represents an individual animal.

Figure 3. Effect of IL-13 on TGF-β$_1$ protein. In A, BAL fluids were obtained from 1–3-mo-old transgene (−) (black bars) and transgene (+) (hatched bars) mice and acid treated. The levels of total TGF-β$_1$ in these fluids were characterized by ELISA. The noted values represent the mean ± SEM of a minimum of four animals. *$P < 0.01$, **$P < 0.001$ versus WT mice. In B, BAL fluids were obtained from 2-mo-old transgene (−) and (+) mice and acid activated. BAL TGF-β$_1$ was then assessed by immunoblot analysis. Each lane represents an individual animal.
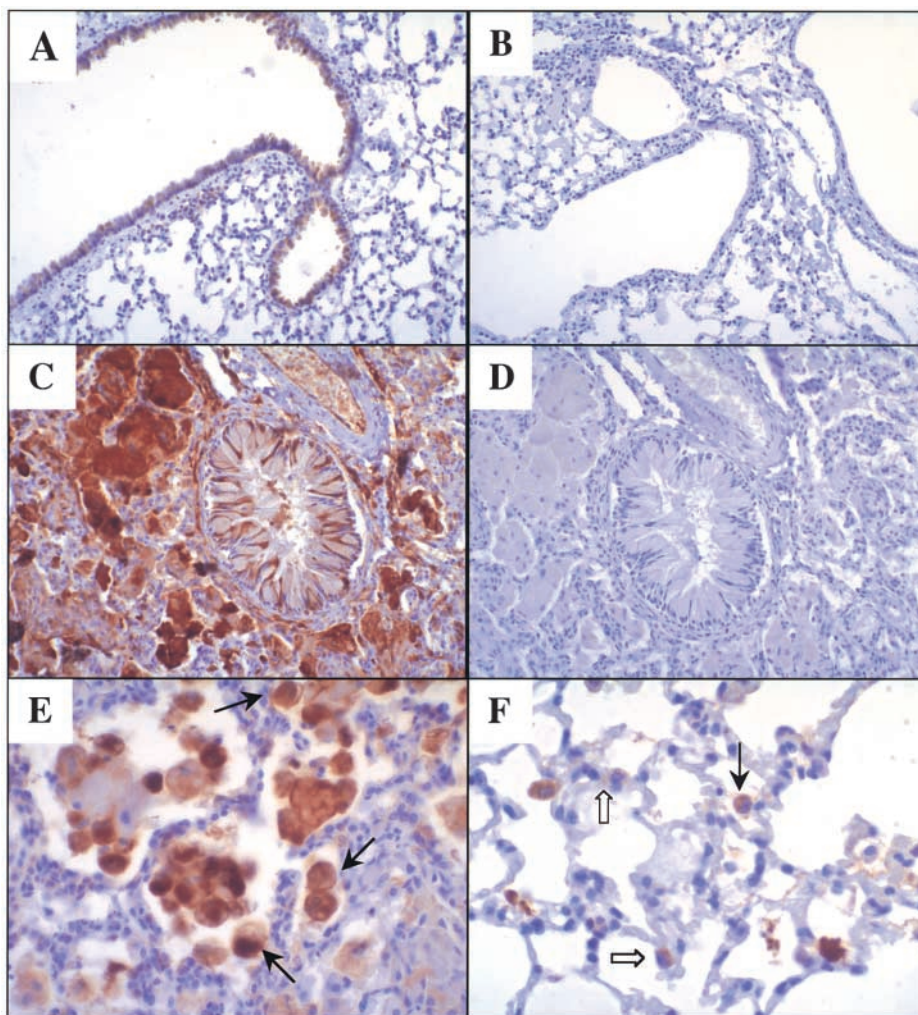
Figure 4. Immunohistochemical localization of TGF-β_1. Immunohistochemistry was used to localize the sites of TGF-β_1 in WT transgene (−) mice and CC10-IL-13 transgene (+) animals (2–3 mo of age). Epithelial TGF-β_1 can be appreciated in the transgene (−) animals (A, original magnification: 20×). Macrophage TGF-β_1 is increased (C, original magnification: 20× and E, original magnification: 40×, black arrows), and alveolar type II epithelial cell (F, original magnification: 40×, white arrows) and eosinophil (F, 40×, black arrow) TGF-β_1 can be appreciated in IL-13 transgene (+) animals. In all cases, preincubation with TGF-β peptide abrogated TGF-β_1 staining (B and D, original magnification: 20×).

in vivo and occurs in biologic fluids in vitro after local acidification (41–45). Studies were thus undertaken to determine if the TGF-β_1 in BAL fluids from IL-13 transgene (+) mice was produced in a biologically inactive or spontaneously activated form. This was done by comparing the TGF-β_1 bioactivities in BAL fluids from transgene (−) and transgene (+) mice using the TMLC/PAI-1 promoter-based luciferase bioassay that only responds to activated TGF-β moieties. As can be seen in Fig. 6, significant TGF-β_1 bioactivity was not present in the untreated or acid-treated BAL fluids from transgene (−) mice. In contrast, impressive levels of spontaneous TGF-β_1 bioactivity were present in untreated BAL fluids from IL-13 transgene (+) animals (Fig. 6 A). Latent TGF-β_1 was also present since acidification revealed an impressive additional increase in the levels of TGF-β_1 bioactivity in BAL fluids from transgene (+) animals (Fig. 6 B). When viewed in combination, these studies demonstrate that IL-13 increases the production and activates TGF-β_1 in the murine lung.

IL-13 Regulation of Processes Involved in TGF-β_1 Activation. Studies were next undertaken to elucidate the mechanism(s) by which IL-13 activated the TGF-β_1 in

lungs from transgene (+) mice. A variety of complex mechanisms of TGF-β_1 activation have been described previously. They include pathways involving CD36 and thombospondin-1 (46, 47), urokinase type plasminogen activator (uPA, and its inhibitor PAI-1) (41, 43, 46, 48, 49), the $\alpha V\beta 6$ integrin (44), latent TGF-β–binding protein (LTBP)-1 (50), and CD44 and MMP-9 (51). To determine if these pathways were activated in IL-13 transgenic mice, we quantitated the levels of mRNA encoding key elements of these pathways in lungs from transgene (−) and transgene (+) animals. Similar levels of mRNA encoding CD36, thombospondin-1, the $\beta 6$ integrin and PAI-1 were seen in whole lung RNA from transgene (−) and transgene (+) animals (Fig. 7). In contrast, an impressive decrease in the levels of mRNA encoding LTBP-1 and significant increases in the levels of mRNA encoding uPA, MMP-9, and CD44 were noted (Fig. 7).

Role of uPA/Serine Proteinases in TGF-β_1 Activation. Because the levels of mRNA encoding uPA were increased in IL-13 transgene (+) animals, studies were undertaken to determine if uPA (or related serine proteinases) played important roles in the activation of TGF-β_1 in lungs from IL-
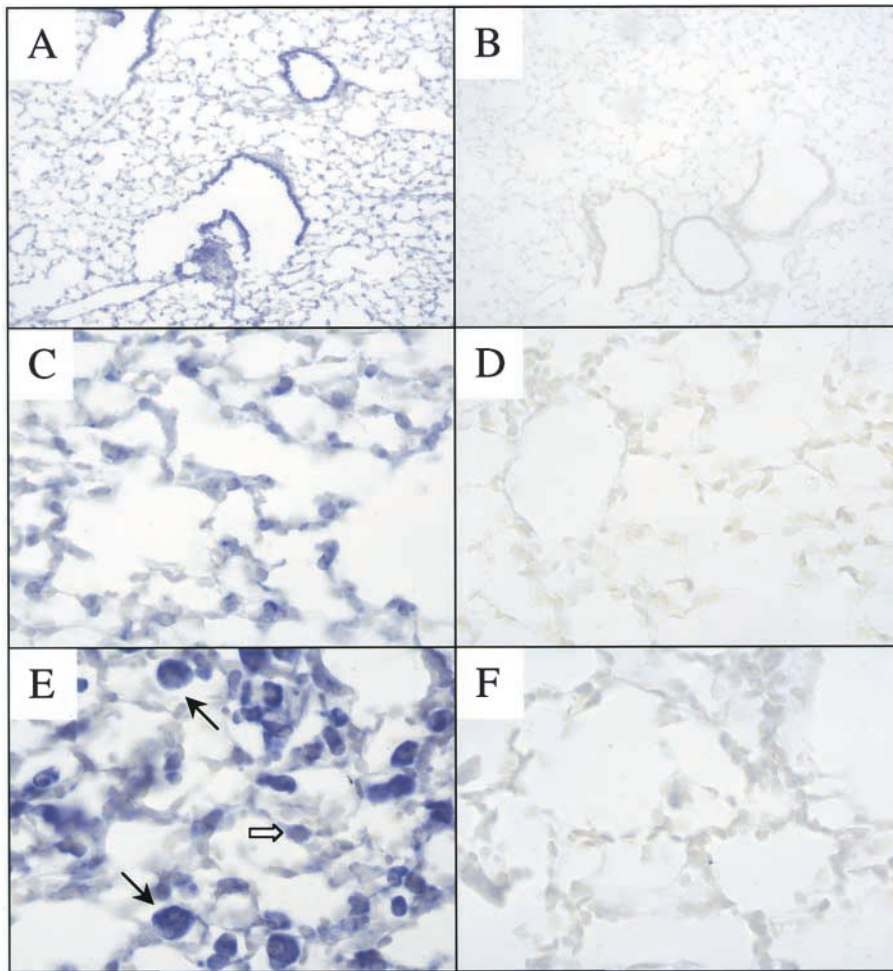
Figure 5. ISHs of TGF-β_1. ISH was used to define the sites of TGF-β_1 mRNA expression in transgene (−) and IL-13 transgene (+) mice (2–3 mo old). Epithelial TGF-β_1 mRNA can be appreciated in the transgene (−) animals (A, original magnification: 10×). Enhanced macrophage (black arrows) and type II alveolar epithelial cell (white arrow) TGF-β_1 mRNA can be seen in comparisons of parenchymal areas from IL-13 transgene (−) mice (C, original magnification: 40×) and transgene (+) mice (E, original magnification: 40×). The lack of staining with the sense probe is seen in B (original magnification: 10×, transgene [−]), D (original magnification: 40×, transgene [−]), and E (original magnification: 40×, transgene [+]).

13 transgene (+) mice. In these experiments we compared the levels of spontaneously bioactive and total TGF-β_1 in BAL fluids from lungs from transgene (+) mice that had been treated with the plasmin/serine proteinase antagonist aprotinin or an appropriate vehicle control. Significant levels of spontaneously active or acid activatable TGF-β_1 were not noted in BAL fluids from transgene (−) mice that received aprotinin or vehicle control (Fig. 8). Aprotinin did, however, totally abrogate the spontaneous activation of TGF-β_1 in BAL fluids from IL-13 transgene (+) mice (Fig. 8). This decrease was out of proportion to the modest decrease in the levels of total TGF-β_1 in the same BAL fluids (Fig. 8). These studies demonstrate that uPA-like serine proteinases, play a critical role in IL-13–induced TGF-β_1 activation in this in vivo system.

Role of MMP-9 and CD44 in IL-13-induced TGF-β_1 Activation. MMP-9 can activate TGF-β cytokines when presented on cell surface CD44 molecules (51). Thus, to define the role of MMP-9 in TGF-β_1 activation, CC10-IL-13 transgene (+) mice were bred with mice with null mutations of MMP-9 or CD44. The spontaneous and total TGF-β_1 bioactivity in BAL fluids from CC10-IL-13 mice with WT and null MMP-9 or CD44 loci were then compared. Spontaneously bioactive TGF-β_1 was not noted in

BAL fluids from WT transgene (−) littermate control animals or animals with null mutations of MMP-9 or CD44 (Fig. 9 and data not shown). As noted above, spontaneously bioactive TGF-β_1 was noted in untreated BAL fluids from CC10-IL-13 transgene (+) mice with WT MMP-9 loci (Fig. 9). Interestingly, null mutations of MMP-9 caused a significant decrease in the levels of spontaneously active TGF-β_1 in BAL fluids from CC10-IL-13 transgene (+) mice (Fig. 9 A). Overall, BAL fluids from CC10-IL-13/ MMP-9$^{−/−}$ mice contained 57 ± 5% as much TGF-β_1 bioactivity as BAL fluids from CC10-IL-13/MMP-9$^{+/+}$ animals ($P < 0.01$). This decrease in TGF-β_1 bioactivity was not due to a decrease in IL-13 elaboration or total TGF-β_1 production since similar levels of BAL IL-13 and acid-activatable total TGF-$\beta_1$were noted in transgene (+) mice with WT and null MMP-9 loci (Fig. 9 B and data not shown). CD44 also did not play an essential role in this MMP-9 effect since similar levels of spontaneously active TGF-β_1 were noted in IL-13 transgenic (+) mice with WT and null CD44 loci (data not shown). These studies demonstrate that MMP-9 plays a critical role in IL-13–induced TGF-β_1 activation, but not in IL-13–induced stimulation of TGF-β_1 production in our transgenic system. They also demonstrate that these TGF-β_1–
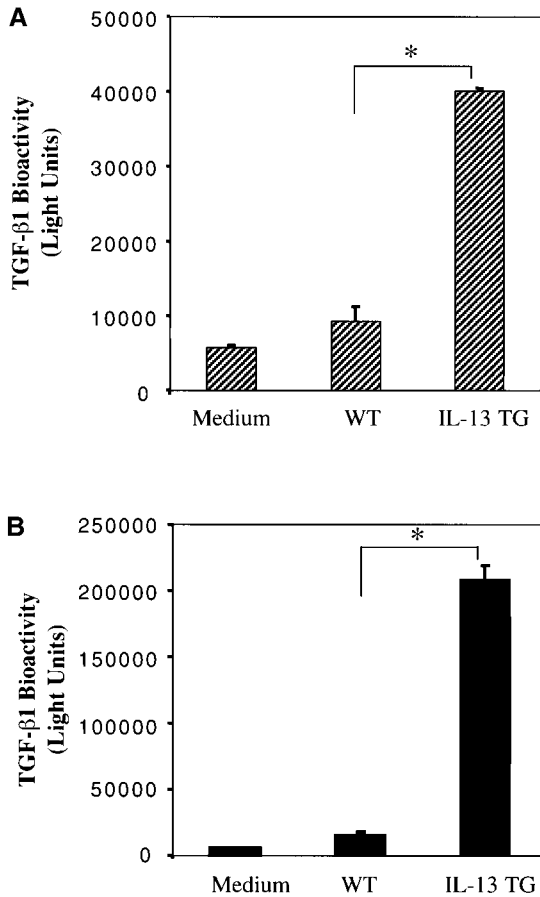
Figure 6. Spontaneous and total TGF-β_1 bioactivity in BAL fluids from transgene ($-$) and transgene ($+$) mice. BAL fluids were obtained from WT transgene ($-$) animals and IL-13 transgene ($+$) (IL-13 TG) mice. The levels of TGF-β_1 bioactivity in these fluids were assessed before (A, spontaneous activity) and after acid activation (B, total activity) using mink lung cells permanently transfected with constructs containing the PAI-1 promoter driving a luciferase reporter gene as described in Materials and Methods. The noted values represent the mean $\pm$ SEM of a minimum of four animals in each category. *$P < 0.001$ versus WT.

activating effects of MMP-9 can be seen in the absence of CD44.

Role of TGF-β_1 and TGF-β_1 Activation in IL-13–induced Fibrosis. Qualitative histologic techniques (trichrome stains), quantitative biochemical approaches, and morphometric assessments of localized collagen deposition were then used to determine if TGF-β_1 played a significant role in IL-13–induced airway and parenchymal fibrosis. In these studies we compared these collagen parameters in IL-13 transgene ($+$) mice that were treated with a TGF-β antagonist (sTGFβR–Fc), aprotinin (which blocks IL-13–induced TGF-β_1 activation), or their appropriate controls. Similar amounts of collagen were noted in lungs from WT littermate control mice that received sTGFβR–Fc, aprotinin, or their respective controls (data not shown). As noted above, IL-13 caused an impressive increase in lung collagen content that could be easily appreciated with all three measurement techniques (Fig. 10 and data not shown). Histologic and biochemical assessments demon-
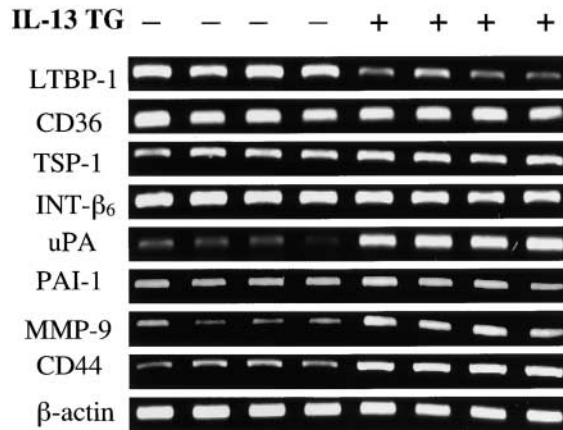

Figure 7. IL-13 regulation of processes involved in TGF-β_1 activation. Whole lung mRNA was obtained from 2–3-mo-old transgene ($-$) and transgene ($+$) mice. The levels of mRNA encoding the noted moieties were evaluated via RT-PCR. Each lane represents an individual animal. The genotype of each animal is noted on the top of the figure.
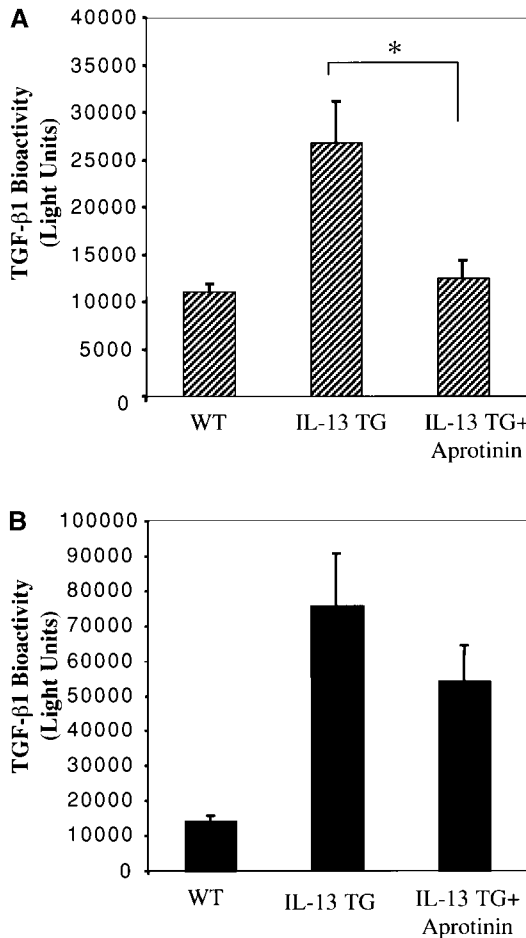

Figure 8. Effect of aprotinin on IL-13-induced TGF-β_1 bioactivity. BAL fluids were obtained from transgene ($+$) mice treated from 1 mo of age to 2 mo of age with aprotinin ($+$ aprotinin) or vehicle control. The spontaneous (A) and acid-activatable (B) TGF-β_1 bioactivity in these fluids are compared to that in BAL fluids from WT transgene ($-$) littermate control animals. The noted values represent the mean $\pm$ SEM of a minimum of four mice in each group. $P < 0.01$.
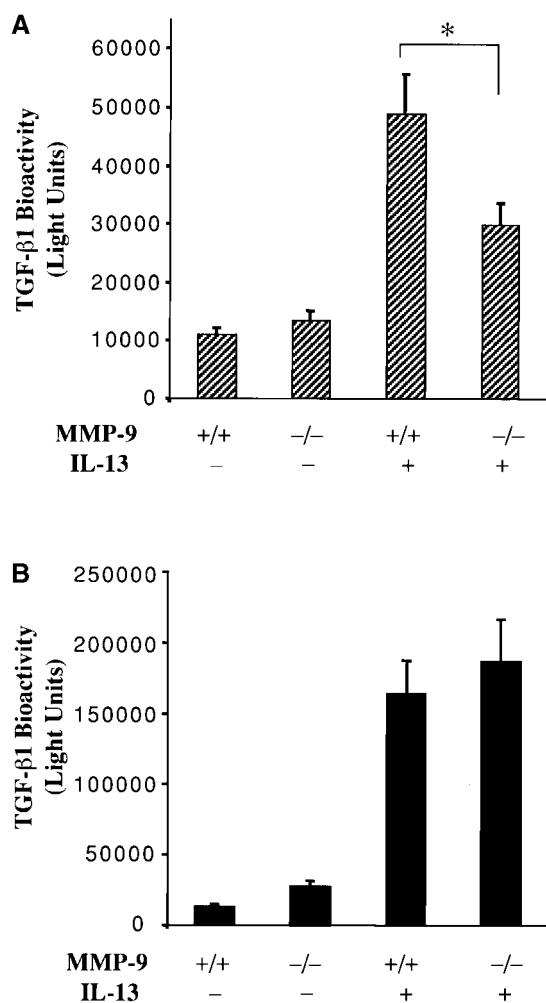
Figure 9. Role of MMP-9 in IL-13 activation and induction of TGF-β_1. BAL fluids were obtained from transgene (−) and transgene (+) CC10-IL-13 mice with WT (+/+) and null (−/−) MMP-9 loci. The levels of spontaneous (A) and total (B) TGF-β_1 bioactivity in these BAL fluids were assessed before and after acid activation respectively as described in Materials and Methods. The noted values represent the mean ± SEM of a minimum of four mice in each group. *$P < 0.01$.

strated that this increase in lung collagen was reduced almost to background levels in CC10-IL-13 mice that received sTGFβR–Fc (Fig. 10). In addition, the Sirius red morphometric evaluations demonstrated that this antifibrotic effect was readily apparent in both the airway and parenchymal tissue compartments where collagen was decreased 85.5 ± 9 and 81.3 ± 11% respectively after sTG-FβR-Fc administration ($P < 0.001$ for both comparisons). Importantly, a significant decrease in collagen content was also seen after aprotinin administration (Fig. 10). Overall, these studies demonstrate, by multiple methods, that TGF-β_1 is the major mediator of IL-13–induced airway and parenchymal fibrosis in our in vivo system. They also demonstrate that this fibrotic response requires TGF-β_1 activation which is mediated, at least in part, by a uPA/ serine protease-dependent mechanism.

Discussion

To further understand the mechanism(s) by which IL-13 generates tissue fibrosis, we took advantage of a transgenic system developed in our laboratory in which the chronic pulmonary overexpression of IL-13 induces airway and parenchymal tissue fibrosis. By comparing the regulation of TGF-β cytokines and related proteins in lungs from transgene (+) mice and transgene (−) littermate controls, and comparing the fibrotic responses induced by IL-13 in animals that received and did not receive TGF-β antagonists, we were able to define the effects of IL-13 on TGF-β cytokines and the role of TGF-β cytokines in IL-13–induced fibrosis. These studies demonstrate that IL-13 is a potent stimulator of TGF-β_1. They also demonstrate that IL-13 activates TGF-β_1 in vivo and that this activation is mediated by a serine protease/plasmin– and MMP-9–dependent mechanism. Lastly, these studies demonstrate that the fibrotic effects of IL-13 are mediated, at least in part, by this TGF-β_1 induction and activation pathway. When viewed in combination, these studies highlight a novel relationship between IL-13 and TGF-β_1 which is likely to play a key role in the pathogenesis of Th2- and IL-13–induced tissue remodeling responses.

Although there are >30 members of the TGF-β supergene family, three moieties (TGF-β_1, TGF-β_2, and TGF-β_3) are the major moieties involved in mammalian regulatory systems (45, 52). These cytokines are products of separate genes that are differentially regulated and expressed (53). As a result, studies were undertaken to determine if IL-13 stimulated these TGF-β moieties in a selective fashion and define the sites of TGF-β_1 production and localization after this induction. These studies demonstrated that TGF-β_1 is the major moiety induced by IL-13 in our animals and that TGF-β_1 mRNA and protein can be found in large quantities in macrophages and lesser quantities in bronchiolar epithelial cells, alveolar type II cells, and eosinophils from these animals. These findings are in accord with studies that demonstrate that TGF-β_1 plays a central role in the pathogenesis of a variety of fibrotic disorders and models of these diseases (35, 45, 54, 55) and studies that demonstrate that macrophages, alveolar epithelial cells, alveolar type II epithelial cells, and eosinophils are important sites of TGF-β_1 production and/or localization in murine models of bleomycin-induced pulmonary fibrosis, human IPF, and human asthma (49, 54–56). It is important to point out that these studies do not rule out a role for TGF-β_2 and/or TGF-β_3 in the pathogenesis of the phenotype of our transgenic mice or in other IL-13–associated fibrotic disorders because TGF-β_2 and TGF-β_3 are expressed in a ubiquitous fashion in normal pulmonary tissues (55).

TGF-β moieties are elaborated by a wide array of hematopoietic and structural cells (53, 57). In these cells, TGF-β_1 is produced as a propeptide which is proteolytically processed into its propeptide fragment (LAP) and a COOH-terminal peptide which forms a disulfide-linked homodimer (43–45, 50, 58). In virtually all cases, TGF-β_1 is elaborated as a biologically inactive latent complex which
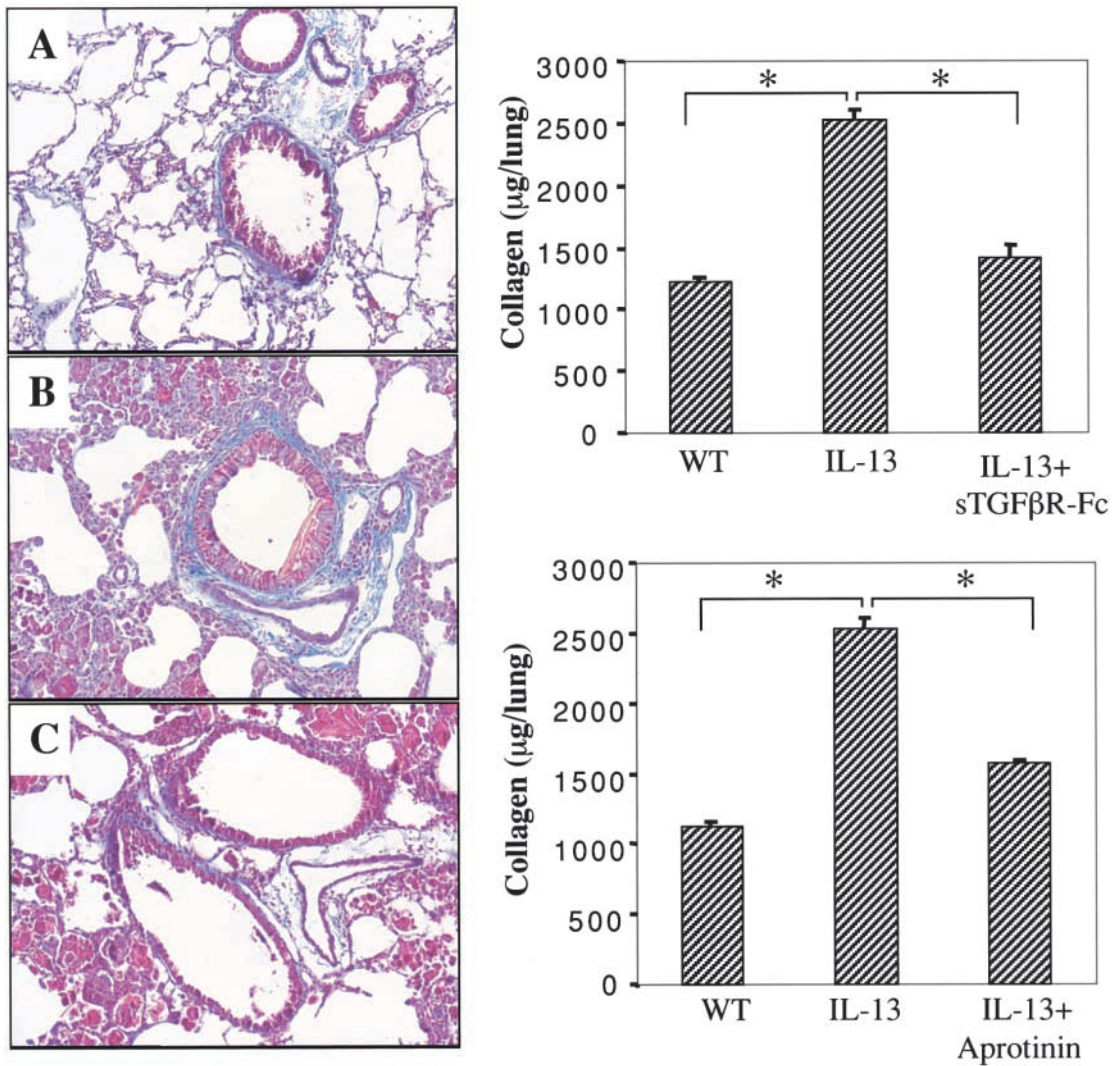
Figure 10. Effects of sTGFβR-Fc and aprotinin on IL-13–induced fibrosis. In the panels on the left 1 mo-old IL-13 transgene (+) mice were treated with sTGFβR-Fc or control and collagen was assessed with trichrome stains. Comparisons are made of WT littermate transgene (−) control mice (A), transgene (+) mice that received control IgG (B), and transgene (+) mice that received sTGFβR-Fc (C). In the panels on the right Sircol biochemical assays were used to characterize the effects of sTGFβR-Fc or aprotinin on lung collagen content. Comparisons are made of WT littermate transgene (−) control mice, transgene (+) mice that received appropriate controls (IL-13) and transgene (+) mice that received sTGFβR-Fc (+ sTGFβR-Fc) or aprotinin (+ aprotinin). Each bar represents the mean ± SEM of a minimum of four animals. *$P < 0.01$.

is formed by the covalent bonding of LAP and the TGF-β dimer and the linking to LTBP-1 (43–45, 50, 58). The amino terminal of LTBP-1 is critical for tissue transglutaminase cross–linking into matrix. Activation of TGF-β_1 is required for TGF-β effector functions to be appreciated. This is accomplished via multiple complex mechanisms that release TGF-β_1 from the matrix and cleave and/or induce conformational changes that allow TGF-β_1 to bind to its receptor (41, 43–45, 50, 58). Decreases in the levels of LTBP-1 (50), plasmin activation (43, 46, 48–50), and pathways involving CD-36 and tissue thrombospondin-1 (46, 47), the αVβ6 integrin (43) and MMP-9 expressed on cell surface CD44 molecules (51) can all play important roles in TGF-β_1 activation. In contrast to the majority of models of pulmonary fibrosis in which only latent TGF-β_1 can be de-

tected in BAL fluids, our studies demonstrate that a significant amount of the TGF-β_1 in the BAL fluids from CC10-IL-13 transgenic mice is spontaneously bioactive. They also demonstrate that the levels of mRNA encoding LTBP-1 are markedly diminished and the levels encoding uPA (which activates plasminogen to bioactive plasmin), MMP-9, and CD44 are increased in IL-13 transgenic mice. This suggests that the decrease in LTBP-1 and the increase in plasmin and MMP-9 play important roles in this activation. Studies using aprotinin corroborated this speculation since this well-known plasmin inhibitor (48, 51, 59) totally abrogated the ability of IL-13 to spontaneously activate TGF-β_1 in the lungs from our transgenic animals. The importance of MMP-9 was also confirmed by breeding the CC10-IL-13 transgene (+) mice with mice with a null mutation of

MMP-9, since the levels of spontaneously bioactive TGF-β_1 in BAL fluids from IL-13 transgene (+) mice with a null MMP-9 locus were significantly lower than the levels in BAL fluids from IL-13 transgene (+) mice with a WT MMP-9 locus. Interestingly, the effects on TGF-β_1 activation of aprotinin exceeded the effects of the MMP-9 null mutation in our transgenic system. uPA-activated plasmin activates MMP-9, both directly and via an indirect pathway that involves MMP-3 (60). TGF-β_1 is also known to stimulate uPA production (61). Thus, the ability of uPA/plasmin to active TGF-β_1 in lungs from IL-13 transgene (+) mice may be mediated, in part, via the ability of plasmin to activate MMP-9. In addition, it is tempting to hypothesize that the LTBP-1, uPA, plasmin, IL-13, and TGF-β_1, in our transgenic animals, are involved in an amplification loop that drives tissue fibrosis. In this schema, IL-13 stimulates TGF-β_1 and MMP-9 production and inhibits LTBP-1. IL-13 also stimulates uPA either directly or via TGF-β_1. The decrease in LTBP-1, increase in uPA-induced plasmin, and increase in MMP-9 all feedback to activate additional TGF-β_1. The TGF-β_1, in turn stimulates the elaboration of additional uPA and activates additional MMP-9 which activates more TGF-β_1. The increased levels of active TGF-β_1 then generate additional tissue fibrosis.

An interesting relationship between the hyaluronan receptor CD44, MMP-9, and TGF-β cytokines has been documented in in vitro studies using tumor cells and normal keratinocytes. In these studies CD44 was shown to provide a docking receptor that localized bioactive MMP-9 to the cell surface, and the CD44-MMP-9 complex was shown to proteolytically activate latent TGF-β moieties (51). To determine if similar mechanisms were operative in vivo, we compared the levels of spontaneously bioactive TGF-β_1 in BAL fluids from IL-13 transgene (+), IL-13$^+$/MMP-9$^{-/-}$, and IL-13$^+$/CD44$^{-/-}$ mice. These studies demonstrated that MMP-9 plays an essential role in IL-13–induced TGF-β activation since significantly decreased levels of spontaneously bioactive TGF-β_1 were noted in BAL fluids from mice with the null MMP-9 mutation. Surprisingly, similar levels of spontaneous TGF-β_1 bioactivity were found in BAL fluids from IL-13 transgene (+) mice with WT (+/+) and null CD44 loci. This demonstrates that MMP-9 does not require CD44 to activate TGF-β_1 in vivo in the lung. This CD44 independence may reflect the ability of other molecules to present active MMP-9 on the surface of cells in this complex in vivo system. Alternatively, MMP-9 may only require CD44 to activate specific TGF-β moieties since, in vitro, TGF-β_2 and TGF-β_3 are more susceptible to activation via the CD44/MMP-9 complex than TGF-β_1 (51).

In early studies, IL-13 was noted to have effector properties that are relevant to Th2 inflammation including the ability to stimulate IgE production, endothelial VCAM-1 expression, and activate B cells (62–64). More recently, IL-13 has been shown to be associated with and induce tissue fibrosis (12, 13, 25). This effect was assumed to be due to direct effects of IL-13 on fibroblasts since IL-13 stimulates fibroblast proliferation and collagen production in vitro

(12, 29, 30). Our studies add to our understanding of this response by demonstrating that IL-13 also stimulates the production and activates TGF-β in vivo. They also demonstrate that IL-13 induces tissue fibrosis, in great extent, via this TGF-β_1 induction and activation pathway. These findings have important implications for diseases such as asthma, IPF, PPS, and hepatic fibrosis which are characterized by IL-13 production, increased TGF-β production, and tissue fibrosis. They suggest that IL-13–stimulated TGF-β_1 production and activation may be a major contributor to the pathogenesis of the tissue fibrosis seen in these diseases. They also suggest that IL-13 stimulation and activation of TGF-β_1 may represent a healing response in the host designed to control and repair IL-13–induced tissue injury. Lastly, they allow for the speculation that interventions that decrease IL-13–induced TGF-β_1 production, TGF-β_1 activation, and/or TGF-β_1 effector functions will have beneficial effects in these and other IL-13–mediated fibrotic diseases. The latter may be especially important since our present therapeutic approaches do not control the tissue fibrosis that is a major contributor to the morbidity and mortality of these disorders.

References

1. Bradding, P., A.E. Redington, and S.T. Holgate. 1997. Airway wall remodelling in the pathogenesis of asthma: cytokine expression in the airways. *In* Airway Wall Remodelling in Asthma. A.G. Stewart, editor. CRC Press, Inc., Boca Raton, FL. 29–63 pp.
2. Ray, A., and L. Cohn. 1999. Th2 cells and GATA-3 in asthma: new insights into the regulation of airway inflammation. *J. Clin. Invest.* 104:1001–1006.
3. Elias, J.A., Z. Zhu, G. Chupp, and R.J. Homer. 1999. Airway remodeling in asthma. *J. Clin. Invest.* 104:1001–1006.
4. Hasegawa, M., M. Fujimoto, K. Kikuchi, and K. Takehara. 1997. Elevated serum levels of interleukin 4 (IL-4), IL-10, and IL-13 in patients with systemic sclerosis. *J. Rheumatol.* 24:328–332.
5. Majumdar, S., D. Li, T. Ansari, P. Pantelidis, C.M. Black, M. Gizycki, R.M. du Bois, and P.K. Jeffery. 1999. Different cytokine profiles in cryptogenic fibrosing alveolitis and fibrosing alveolitis associated with systemic sclerosis. *Eur. Respir. J.* 14:251–257.
6. Romagnani, S. 1999. Th1/Th2 cells. *Inflamm. Bowel Dis.* 5:285–294.
7. Wallace, W.A., E.A. Ramage, D. Lamb, and S.D. Howie. 1995. A type 2 (Th2-like) pattern of immune response predominates in the pulmonary interstitium of patients with

cryptogenic fibrosing alveolitis (CFA). *Clin. Exp. Immunol.* 101:436–441.

8. Ziesche, R., E. Hofbauer, K. Wittmann, V. Petkov, and L.H. Block. 1999. A preliminary study of long term treatment with interferon γ-1β and low dose prednisolone in patients with idiopathic pulmonary fibrosis. *New Engl. J. Med.* 341: 1264–1269.

9. Westermann, W., R. Schobl, E.P. Rieber, and K.H. Frank. 1999. Th2 cells as effectors in postirradiation pulmonary damage preceding fibrosis in the rat. *Int. J. Radiat. Biol.* 75: 629–638.

10. Shirwan, H. 1999. Chronic allograft rejection. Do the Th2 cells preferentially induced by indirect alloantigen recognition play a dominant role? *Transplantation.* 68:715–726.

11. Gharaee-Kermani, M., and S. Phan. 1997. Lung interleukin-5 expression in murine bleomycin-induced pulmonary fibrosis. *Am. J. Resp. Cell. Mol. Biol.* 16:438–447.

12. Chiramonte, M.G., D.D. Donaldson, A.W. Cheever, and T.A. Wynn. 1999. An IL-13 inhibitor blocks the development of hepatic fibrosis during a T-helper type 2-dominated inflammatory response. *J. Clin. Invest.* 104:777–785.

13. Fallon, P.G., E.J. Richardson, G.J. McKenzie, and A.N. McKenzie. 2000. Schistosome infection of transgenic mice defines distinct and contrasting pathogenic roles for IL-4 and IL-13: IL-13 is a profibrotic agent. *J. Immunol.* 164:2585–2591.

14. Hoffmann, K.F., A.W. Cheever, and T.A. Wynn. 2000. IL-10 and the dangers of immune polarization: excessive type 1 and type 2 cytokine responses induce distinct forms of lethal immunopathology in murine schistosomiasis. *J. Immunol.* 164:6406–6416.

15. Shi, Z., A.E. Wakil, and D.C. Rockey. 1997. Strain-specific differences in mouse hepatic wound healing are mediated by divergent T helper cytokine responses. *Cell Biol.* 94:10663–10668.

16. Wangoo, A., T. Sparer, I.N. Brown, V.A. Snewin, R. Janssen, J. Thole, H.T. Cook, R.J. Shaw, and D.B. Young. 2001. Contribution of Th1 and Th2 cells to protection and pathology in experimental models of granulomatous lung disease. *J. Immunol.* 166:3432–3439.

17. Gurujeyalakshmi, G., and S.N. Giri. 1995. Molecular mechanisms of antifibrotic effect of interferon γ in bleomycin-mouse model of lung fibrosis: downregulation of TGF-β and procollagen I and III gene expression. *Exp. Lung Res.* 21: 791–808.

18. Oldroyd, S.D., G.L. Thomas, G. Gabiani, and A.M. El Nahas. 1999. Interferon-γ inhibits experimental renal fibrosis. *Kidney Int.* 56:2116–2127.

19. Sime, P.J., and K.M.A. O'Reily. 2001. Fibrosis in the lung and other tissues: new concepts in pathogenesis and treatment. *Clin. Immunol.* 99:308–319.

20. de Vries, J.E. 1998. The role of IL-13 and its receptor in allergy and inflammatory responses. *J. Allergy Clin. Immunol.* 102:165–169.

21. Minty, A., S. Asselin, A. Bensussan, D. Shire, N. Vita, A. Vyakarnam, J. Wijdenes, P. Ferrara, and D. Caput. 1997. The related cytokines interleukin-13 and interleukin-4 are distinguished by differential production and differential effects on T lymphocytes. *Eur. Cytokine Netw.* 8:203–213.

22. Grünig, G., M. Warnock, A.E. Wakil, R. Venkayya, F. Brombacher, D.M. Rennick, D. Sheppard, M. Mohrs, D.D. Donaldson, R.M. Locksley, and D.B. Corry. 1998. Requirement for IL-13 independently of IL-4 in experimental asthma. *Science.* 282:2261–2263.

23. Kotsimbos, T.C., P. Ernst, and Q.A. Hamid. 1996. Interleukin-13 and interleukin-4 are coexpressed in atopic asthma. *Proc. Assoc. Am. Physicians.* 108:368–373.

24. Wills-Karp, M., J. Luyimbazi, X. Xu, B. Schofield, T.Y. Neben, C.L. Karp, and D.D. Donaldson. 1998. Interleukin-13: central mediator of allergic asthma. *Science.* 282:2258–2260.

25. Zhu, Z., R.J. Homer, Z. Wang, Q. Chen, G.P. Geba, J. Wang, Y. Zhang, and J.A. Elias. 1999. Pulmonary expression of interleukin-13 causes inflammation, mucus hypersecretion, subepithelial fibrosis, physiologic abnormalities and eotaxin production. *J. Clin. Invest.* 103:779–788.

26. Chiaramonte, M.G., L.R. Schopf, T.Y. Neben, A.W. Cheever, D.D. Donaldson, and T.A. Wynn. 1999. IL-13 is a key regulatory cytokine for Th2 cell-mediated pulmonary granuloma formation and IgE responses induced by *Schistosoma mansoni* eggs. *J. Immunol.* 162:920–930.

27. Hancock, A., L. Armstrong, R. Gama, and A. Millar. 1998. Production of interleukin 13 by alveolar macrophages from normal and fibrotic lung. *Am. J. Respir. Cell Mol. Biol.* 18:60–65.

28. Ohshima, K., M. Akaiwa, R. Umeshita, J. Suzumiya, K. Izuhara, and M. Kikuchi. 2001. Interleukin-13 and interleukin-13 receptor in Hodgkin's disease: possible autocrine mechanism and involvement in fibrosis. *Hostopathology.* 38: 368–375.

29. Doucet, C., D. Brouty-Boye, C. Pottin-Clemenceau, G.W. Canonica, C. Jasmin, and B. Azzarone. 1998. Interleukin (IL)-4 and IL-13 act on human lung fibroblasts. *J. Clin. Invest.* 101:2129–2139.

30. Oriente, A., N.S. Fedarko, S.E. Pacocha, S.K. Huang, L.M. Lichtenstein, and D.M. Essayan. 2000. Interleukin-13 modulates collagen homeostasis in human skin and keloid fibroblasts. *J. Pharmacol. Exp. Ther.* 292:988–994.

31. Vu, T.H., J.M. Shipley, G. Bergers, J.E. Berger, J.A. Helms, D. Hanahan, S.D. Shapiro, R.M. Senior, and Z. Werb. 1998. MMP-9/gelatinase B is a key regulator of growth plate angiogenesis and apoptosis of hypertrophic chondrocytes. *Cell.* 93:411–422.

32. Schmits, R., J. Filmus, N. Gerwin, G. Senaldi, F. Kiefer, T. Kundig, A. Wakeham, A. Shahinian, C. Catzavelos, J. Rak, et al. 1997. CD44 regulates hematopoietic progenitor distribution, granuloma formation, and tumorigenicity. *Blood.* 90: 2217–2233.

33. Zheng, T., Z. Zhu, Z. Wang, R.J. Homer, B. Ma, R. Riese, H. Chapman, S.D. Shapiro, and J.A. Elias. 2000. Inducible targeting of IL-13 to the adult lung causes matrix metalloproteinase- and cathepsin-dependent emphysema. *J. Clin. Invest.* 106:1081–1093.

34. Tang, W., G.P. Geba, T. Zheng, P. Ray, R. Homer, C. Kuhn, R.A. Favell, and J.A. Elias. 1996. Targeted expression of IL-11 in the murine airway causes airways obstruction, bronchial remodeling and lymphocytic inflammation. *J. Clin. Invest.* 98:2845–2853.

35. George, J., D. Roulot, V.E. Koteliansky, and D.M. Bissell. 1999. In vivo inhibition of rat stellate cell activation by soluble transforming growth factor β type II receptor: a potential new therapy for hepatic fibrosis. *Proc. Natl. Acad. Sci. USA.* 96:12719–12724.

36. Smith, J.D., S.R. Bryant, L.L. Couper, C.P. Vary, P.J. Gotwals, V.E. Koteliansky, and V. Lindner. 1999. Soluble transforming growth factor-β type II receptor inhibits negative

remodeling, fibroblast transdifferentiation, and intimal lesion formation but not endothelial growth. *Circ. Res.* 84:1212–1222.

37. Wang, J.M., R.J. Homer, L. Hong, L. Cohn, C.G. Lee, and J.A. Elias. 2000. IL-11 selectively inhibits aeroallergen-induced pulmonary eosinophilia and Th2 cytokine production. *J. Immunol.* 165:2222–2231.

38. Bosch, J.J., K.S. Zyderhoudt, F.M. Houtkooper, and J. van Gool. 1986. Histophotometric estimation of volume density of collagen as an indication of fibrosis in rat liver. *Histochemistry.* 85:129–133.

39. Ashcroft, G.S., K. Lei, W. Jin, G. Longnecker, A.B. Kulkarnt, T. Greenwell-Wild, H. Hale-Donze, G. McGrady, X.-Y. Song, and S.M. Wahl. 2000. Secretory leukocyte protease inhibitor mediates non-redundant functions necessary for wound healing. *Nat. Med.* 6:1147–1153.

40. Junqueira, L.C., G. Bignolas, and R.R. Brentani. 1979. Picrosirius staining plus polarization microscopy, a specific method for collagen detection in tissue sections. *Histochem. J.* 11:447–455.

41. Khalil, N. 1999. TGF-β: from latent to active. *Microbes. Infect.* 1:1255–1263.

42. Khalil, N. 2001. Post translational activation of latent transforming growth factor β (L-TGF-β): Clinical implications. *Histol. Histopathol.* 16:541–551.

43. Munger, J.S., J.G. Harpel, P.E. Gleizes, R. Mazzieri, I. Nunes, and D.B. Rifkin. 1997. Latent transforming growth factor-β: structural features and mechanisms of activation. *Kidney Intl.* 51:1376–1382.

44. Munger, J.S., X. Huang, H. Kawakatsu, M.J. Griffiths, S.L. Dalton, J. Wu, J.F. Pittet, N. Kaminski, C. Garat, M.A. Matthay, et al. 1999. The integrin αvβ6 binds and activates latent TGF β1: a mechanism for regulating pulmonary inflammation and fibrosis. *Cell.* 96:319–328.

45. Clark, D.A., and R. Coker. 1998. Transforming growth factor-β (TGF-β). *Int. J. Biochem. Cell Biol.* 30:293–298.

46. Yehualaeshet, T., R. O'Connor, J. Green-Johnson, S. Mai, R. Silverstein, J.E. Murphy-Ullrich, and N. Khalil. 1999. Activation of rat alveolar macrophage-derived latent transforming growth factor β-1 by plasmin requires interaction with thrombospondin-1 and its cell surface receptor, CD36. *Am. J. Pathol.* 155:841–851.

47. Yehualaeshet, T., R. O'Connor, A. Begleiter, J.E. Murphy-Ullrich, R. Silverstein, and N. Khalil. 2000. A CD36 synthetic peptide inhibits bleomycin-induced pulmonary inflammation and connective tissue synthesis in the rat. *Am. J. Respir. Cell Mol. Biol.* 23:204–212.

48. Herbert, J.M., and P. Carmeliet. 1997. Involvement of u-PA in the antiapoptotic activity of TGF-beta for vascular smooth muscle cells. *FEBS Lett.* 413:401–404.

49. Khalil, N., S. Corne, C. Whitman, and H. Yacyshyn. 1996. Plasmin regulates the activation of cell-associated latent TGF-β1 secreted by rat alveolar macrophages after in vivo bleomycin injury. *Am. J. Respir. Cell Mol. Biol.* 15:252–259.

50. Rifkin, D.B., R. Mazzieri, J.S. Munger, I. Noguera, and J. Sung. 1999. Proteolytic control of growth factor availability. *APMIS.* 107:80–85.

51. Yu, Q., and I. Stamenkovic. 2000. Cell surface-localized matrix metalloproteinase-9 proteolytically activates TGF-β and promotes tumor invasion and angiogenesis. *Genes and Develop.* 14:163–176.

52. Shah, M., D. Revis, S. Herrick, R. Baillie, S. Thorgeirson, M. Ferguson, and A. Roberts. 1999. Role of elevated plasma transforming growth factor-β1 levels in wound healing. *Am. J. Pathol.* 154:1115–1124.

53. Letterio, J.L., and A.B. Roberts. 1998. Regulation of immune responses by TGF-β. *Annu. Rev. Immunol.* 16:137–161.

54. Khalil, N., R.N. O'Connor, H.W. Unruh, P.W. Warren, K.C. Flanders, A. Kemp, O.H. Bereznay, and A.H. Greenberg. 1991. Increased production and immunohistochemical localization of transforming growth factor-β in idiopathic pulmonary fibrosis. *Am. J. Respir.Cell Mol. Biol.* 5:155–162.

55. Khalil, N., R.N. O'Connor, K.C. Flanders, and H. Unruh. 1996. TGF-β1, but not TGF-β2 or TGF-β3, is differentially present in epithelial cells of advanced pulmonary fibrosis: an immunohistochemical study. *Am. J. Respir. Cell Mol. Biol.* 14:131–138.

56. Minshall, E.M., D.Y. Leung, R.J. Martin, Y.L. Song, L. Cameron, P. Ernst, and Q. Hamid. 1997. Eosinophil-associated TGF-β1 mRNA expression and airways fibrosis in bronchial asthma. *Am. J. Respir. Cell Mol. Biol.* 17:326–333.

57. Letterio, J.J., and A.B. Roberts. 1997. Molecule of the month. TGF-β: a critical modulator of immune cell function. *Clin. Immunol. Immunopath.* 84:244–250.

58. Macatonia, S.E., N.A. Hosken, M. Litton, P. Vieira, C. Hsieh, J.A. Culpepper, M. Wysocka, G. Trinchieri, K.M. Murphy, and A. O'Garra. 1995. Dendritic cells produce IL-12 and direct the development of Th1 cells from naive CD4+ T cells. *J. Immunol.* 154:5071–5079.

59. Davis, G.E., K.A. Pintar Allen, R. Salazar, and S.A. Maxwell. 2001. Matrix metalloproteinase-1 and -9 activation by plasmin regulates a novel endothelial cell–mediated mechanism of collagen gel contraction and capillary tube regression in three dimensional collagen matrices. *J. Cell Sci.* 114:917–930.

60. Ramos-DeSimone, N., E. Hahn-Datona, J. Sipley, H. Nagase, D.L. French, and J.P. Quigley. 1999. Activation of matrix metalloproteinase-9 (MMP-9) via a converging plasmin/stromolysin-1 cascade enhances tumor cell invasion. *J. Biol. Chem.* 274:13066–13076.

61. Santibanez, J.F., M. Iglesias, P. Frontello, J. Martinez, and M. Quintinilla. 2000. Involvement of the Ras/MAPK signaling pathway in the modulation of urokinase production and cellular invasiveness by transforming growth factor-β1 in transformed keratinocytes. *Biochem. Biophys. Res. Comm.* 273:521–527.

62. Emson, C.L., S.E. Bell, A. Jones, W. Wisden, and A.N.J. McKenzie. 1998. Interleukin (IL)-4-independent induction of immunoglobulin (Ig)E, and perturbation of T cell development in transgenic mice expressing IL-13. *J. Exp. Med.* 188:399–404.

63. Zurawski, G., and J.E. de Vries. 1994. Interleukin-13, an interleukin-4-like cytokine that acts on monocytes and B cells, but not on T cells. *Immunol. Today.* 15:19–26.

64. Bochner, B.S., D.A. Klunk, S.A. Sterbinsky, R.L. Coffman, and R.P. Schleimer. 1995. IL-13 selectively induces vascular cell adhesion molecule-1 expression in human endothelial cells. *J. Immunol.* 154:799–803.